Chiral tunnelling and the Klein paradox in graphene

M. I. KATSNELSON[1]*, K. S. NOVOSELOV[2] AND A. K. GEIM[2]*

[1]Institute for Molecules and Materials, Radboud University Nijmegen, 6525 ED Nijmegen, The Netherlands
[2]Manchester Centre for Mesoscience and Nanotechnology, University of Manchester, Manchester M13 9PL, UK
*e-mail: katsnelson@science.ru.nl; geim@manchester.ac.uk

Published online: 20 August 2006; doi:10.1038/nphys384

The so-called Klein paradox—unimpeded penetration of relativistic particles through high and wide potential barriers—is one of the most exotic and counterintuitive consequences of quantum electrodynamics. The phenomenon is discussed in many contexts in particle, nuclear and astro-physics but direct tests of the Klein paradox using elementary particles have so far proved impossible. Here we show that the effect can be tested in a conceptually simple condensed-matter experiment using electrostatic barriers in single- and bi-layer graphene. Owing to the chiral nature of their quasiparticles, quantum tunnelling in these materials becomes highly anisotropic, qualitatively different from the case of normal, non-relativistic electrons. Massless Dirac fermions in graphene allow a close realization of Klein's gedanken experiment, whereas massive chiral fermions in bilayer graphene offer an interesting complementary system that elucidates the basic physics involved.

The term Klein paradox[1–7] refers to a counterintuitive relativistic process in which an incoming electron starts penetrating through a potential barrier if its height, V_0, exceeds the electron's rest energy, mc^2 (where m is the electron mass and c is the speed of light). In this case, the transmission probability, T, depends only weakly on the barrier height, approaching the perfect transparency for very high barriers, in stark contrast to the conventional, non-relativistic tunnelling where T exponentially decays with increasing V_0. This relativistic effect can be attributed to the fact that a sufficiently strong potential, being repulsive for electrons, is attractive for positrons and results in positron states inside the barrier, which align in energy with the electron continuum outside[4–6]. Matching between electron and positron wavefunctions across the barrier leads to the high-probability tunnelling described by the Klein paradox[7]. The essential feature of quantum electrodynamics (QED) responsible for the effect is the fact that states at positive and negative energies (electrons and positrons) are intimately linked (conjugated), being described by different components of the same spinor wavefunction. This fundamental property of the Dirac equation is often referred to as the charge-conjugation symmetry. Although Klein's gedanken experiment is now well understood, the notion of paradox is still widely used[2–7], perhaps because the effect has never been observed experimentally. Indeed, its observation requires a potential drop of $\approx mc^2$ over the Compton length $\hbar/mc$, which yields enormous electric fields[2,3] ($\varepsilon > 10^{16}\,\mathrm{V\,cm^{-1}}$) and makes the effect relevant only for such exotic situations as, for example, positron production around super-heavy nuclei[2,3] with charge $Z \geq 170$ or evaporation of black holes through generation of particle–antiparticle pairs near the event horizon[8]. The purpose of this paper is to show that graphene—a recently found allotrope of carbon[9]—provides an effective medium ('vacuum') where relativistic quantum tunnelling described by the Klein paradox and other relevant QED phenomena can be tested experimentally.

DIRAC-LIKE QUASIPARTICLES IN GRAPHENE

Graphene is a single layer of carbon atoms densely packed in a honeycomb lattice, or it can be viewed as an individual atomic plane pulled out of bulk graphite. From the point of view of

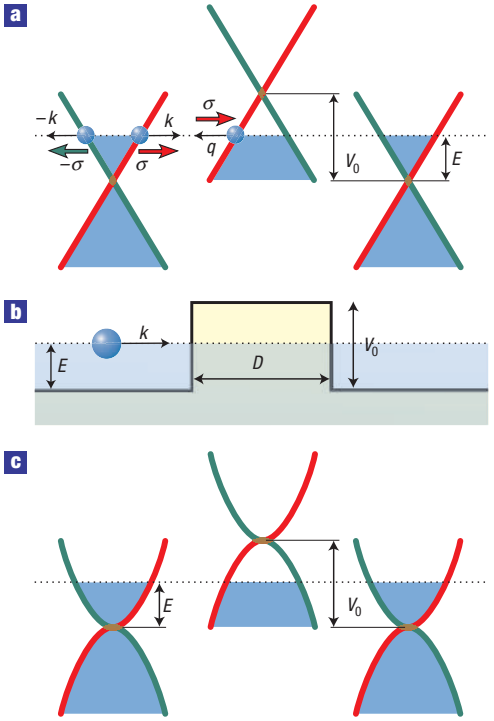

Figure 1 Tunnelling through a potential barrier in graphene. a, Schematic diagrams of the spectrum of quasiparticles in single-layer graphene. The spectrum is linear at low Fermi energies (<1 eV). The red and green curves emphasize the origin of the linear spectrum, which is the crossing between the energy bands associated with crystal sublattices A and B. **b**, Potential barrier of height V_0 and width D. The three diagrams in **a** schematically show the positions of the Fermi energy E across such a barrier. The Fermi level (dotted lines) lies in the conduction band outside the barrier and the valence band inside it. The blue filled areas indicate occupied states. The pseudospin denoted by vector σ is parallel (antiparallel) to the direction of motion of electrons (holes), which also means that σ keeps a fixed direction along the red and green branches of the electronic spectrum. **c**, Low-energy spectrum for quasiparticles in bilayer graphene. The spectrum is isotropic and, despite its parabolicity, also originates from the intersection of energy bands formed by equivalent sublattices, which ensures charge conjugation, similar to the case of single-layer graphene.

its electronic properties, graphene is a two-dimensional zero-gap semiconductor with the energy spectrum shown in Fig. 1a, and its low-energy quasiparticles are formally described by the Dirac-like hamiltonian[10–12]

$$\widehat{H}_0 = -i\hbar v_F \sigma \nabla, \qquad (1)$$

where $v_F \approx 10^6\ \mathrm{m\,s^{-1}}$ is the Fermi velocity and $\sigma = (\sigma_x, \sigma_y)$ are the Pauli matrices. Neglecting many-body effects, this description is accurate theoretically[10–12] and has also been proved experimentally[13,14] by measuring the energy-dependent cyclotron mass in graphene (which yields its linear energy spectrum) and, most clearly, by the observation of a relativistic analogue of the integer quantum Hall effect.

The fact that charge carriers in graphene are described by the Dirac-like equation (1), rather than the usual Schrödinger equation, can be seen as a consequence of graphene's crystal structure, which consists of two equivalent carbon sublattices[10–12], A and B. Quantum mechanical hopping between the sublattices leads to the formation of two cosine-like energy bands, and their intersection near the edges of the Brillouin zone (shown in red and green in Fig. 1a) yields the conical energy spectrum. As a result, quasiparticles in graphene exhibit the linear dispersion relation $E = \hbar k v_F$, as if they were massless relativistic particles with momentum k (for example, photons) but the role of the speed of light is played here by the Fermi velocity $v_F \approx c/300$. Owing to the linear spectrum, it is expected that graphene's quasiparticles will behave differently from those in conventional metals and semiconductors where the energy spectrum can be approximated by a parabolic (free-electron-like) dispersion relation.

Although the linear spectrum is important, it is not the only essential feature that underpins the description of quantum transport in graphene by the Dirac equation. Above zero energy, the current carrying states in graphene are, as usual, electron-like and negatively charged. At negative energies, if the valence band is not full, its unoccupied electronic states behave as positively charged quasiparticles (holes), which are often viewed as a condensed-matter equivalent of positrons. Note, however, that electrons and holes in condensed-matter physics are normally described by separate Schrödinger equations, which are not in any way connected (as a consequence of the Seitz sum rule[15], the equations should also involve different effective masses). In contrast, electron and hole states in graphene are interconnected, exhibiting properties analogous to the charge-conjugation symmetry in QED[10–12]. For the case of graphene, the latter symmetry is a consequence of its crystal symmetry because graphene's quasiparticles have to be described by two-component wavefunctions, which are needed to define relative contributions of sublattices A and B in quasiparticles' make-up. The two-component description for graphene is very similar to the one by spinor wavefunctions in QED, but the 'spin' index for graphene indicates sublattices rather than the real spin of electrons and is usually referred to as pseudospin σ.

There are further analogies with QED. The conical spectrum of graphene is the result of intersection of the energy bands originating from sublattices A and B (see Fig. 1a) and, accordingly, an electron with energy E propagating in the positive direction originates from the same branch of the electronic spectrum (shown in red) as the hole with energy $-E$ propagating in the opposite direction. This yields that electrons and holes belonging to the same branch have pseudospin σ pointing in the same direction, which is parallel to the momentum for electrons and antiparallel for holes (see Fig. 1a). This allows the introduction of chirality[12], that is formally a projection of pseudospin on the direction of motion, which is positive and negative for electrons and holes, respectively. The term chirality is often used to refer to the additional built-in symmetry between electron and hole parts of graphene's spectrum (as indicated by colour in Fig. 1) and is analogous (although not completely identical[11,16]) to the chirality in three-dimensional QED.

KLEIN PARADOX REFORMULATED FOR SINGLE-LAYER GRAPHENE

Because quasiparticles in graphene accurately mimic Dirac fermions in QED, this condensed-matter system makes it possible to set up a tunnelling experiment similar to that analysed by Klein. The general scheme of such an experiment is shown in Fig. 1, where we consider the potential barrier that has a rectangular shape and is infinite along the y axis:

$$V(x) = \begin{cases} V_0, & 0 < x < D, \\ 0 & \text{otherwise.} \end{cases} \qquad (2)$$

This local potential barrier of width D inverts charge carriers underneath it, creating holes playing the role of positrons, or

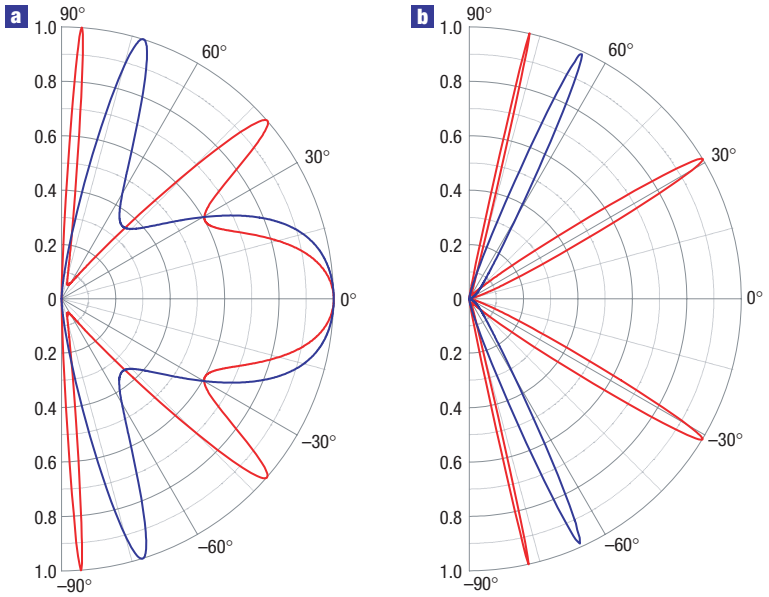

Figure 2 Klein-like quantum tunnelling in graphene systems. a,**b**, Transmission probability T through a 100-nm-wide barrier as a function of the incident angle for single- (**a**) and bi-layer (**b**) graphene. The electron concentration n outside the barrier is chosen as 0.5×10^{12} cm^{-2} for all cases. Inside the barrier, hole concentrations p are 1×10^{12} and 3×10^{12} cm^{-2} for red and blue curves, respectively (such concentrations are most typical in experiments with graphene). This corresponds to the Fermi energy E of incident electrons $\approx$80 and 17 meV for single- and bi-layer graphene, respectively, and $\lambda\approx50$ nm. The barrier heights V_0 are (**a**) 200 and (**b**) 50 meV (red curves) and (**a**) 285 and (**b**) 100 meV (blue curves).

vice versa. For simplicity, we assume in (2) infinitely sharp edges, which allows a direct link to the case usually considered in QED[1–7]. The sharp-edge assumption is justified if the Fermi wavelength, λ, of quasiparticles is much larger than the characteristic width of the edge smearing, which in turn should be larger than the lattice constant (to disallow Umklapp scattering between different valleys in graphene)[17]. Such a barrier can be created by the electric field effect using a thin insulator or by local chemical doping[9,13,14]. Importantly, Dirac fermions in graphene are massless and, therefore, there is no formal theoretical requirement for the minimal electric field, ε, to form positron-like states under the barrier. To create a well-defined barrier in realistic graphene samples with a disorder, fields $\varepsilon\approx10^5$ V cm^{-1} routinely used in experiments[9,14] should be sufficient, which is eleven orders of magnitude lower than the fields necessary for the observation of the Klein paradox for elementary particles.

It is straightforward to solve the tunnelling problem shown in Fig. 1b. We assume that the incident electron wave propagates at an angle ϕ with respect to the x axis and then try the components of the Dirac spinor ψ_1 and ψ_2 for the hamiltonian $H=H_0+V(x)$ in the following form:

$$\psi_1(x,y) = \begin{cases} (e^{ik_x x}+re^{-ik_x x})e^{ik_y y}, & x<0,\\ (ae^{iq_x x}+be^{-iq_x x})e^{ik_y y}, & 0<x<D,\\ te^{ik_x x+ik_y y}, & x>D, \end{cases}$$

$$\psi_2(x,y) = \begin{cases} s(e^{ik_x x+i\phi}-re^{-ik_x x-i\phi})e^{ik_y y}, & x<0,\\ s'(ae^{iq_x x+i\theta}-be^{-iq_x x-i\theta})e^{ik_y y}, & 0<x<D,\\ ste^{ik_x x+ik_y y+i\phi}, & x>D, \end{cases}$$

where $k_F=2\pi/\lambda$ is the Fermi wavevector, $k_x=k_F\cos\phi$ and $k_y=k_F\sin\phi$ are the wavevector components outside the barrier, $q_x=\sqrt{(E-V_0)^2/\hbar^2v_F^2-k_y^2}$, $\theta=\tan^{-1}(k_y/q_x)$ is the refraction angle, $s=\operatorname{sgn}E$ and $s'=\operatorname{sgn}(E-V_0)$. Requiring the continuity of the wavefunction by matching up coefficients a,b,t,r, we find the following expression for the reflection coefficient r

$$r = 2ie^{i\phi}\sin(q_xD)\times\frac{\sin\phi-ss'\sin\theta}{ss'[e^{-iq_xD}\cos(\phi+\theta)+e^{iq_xD}\cos(\phi-\theta)]-2i\sin(q_xD)}. \quad (3)$$

Figure 2a shows examples of the angular dependence of transmission probability $T=|t|^2=1-|r|^2$ calculated using the above expression. In the limit of high barriers $|V_0|\gg|E|$, the expression for T can be simplified to

$$T=\frac{\cos^2\phi}{1-\cos^2(q_xD)\sin^2\phi}. \quad (4)$$

Equations (3) and (4) yield that under resonance conditions $q_xD=\pi N$, $N=0,\pm1,\ldots$ the barrier becomes transparent ($T=1$). More significantly, however, the barrier always remains perfectly transparent for angles close to the normal incidence $\phi=0$. The latter is the feature unique to massless Dirac fermions and is directly related to the Klein paradox in QED. This perfect tunnelling can be understood in terms of the conservation of pseudospin. Indeed, in the absence of pseudospin-flip processes (such processes are rare as they require a short-range potential, which would act differently on A and B sites of the graphene lattice), an electron moving to the right can be scattered only to a right-moving electron state or left-moving hole state. This is shown in Fig. 1a, where charge carriers from the 'red' branch of the band diagram can be scattered into states within the same 'red' branch but cannot be transformed into any state on the 'green' branch. The latter scattering event would require the pseudospin to be flipped. The

matching between directions of pseudospin σ for quasiparticles inside and outside the barrier results in perfect tunnelling. In the strictly one-dimensional case, such perfect transmission of Dirac fermions has been discussed in the context of electron transport in carbon nanotubes[17,18] (see also ref. 19). Our analysis extends this tunnelling problem to the two-dimensional (2D) case of graphene.

CHIRAL TUNNELLING IN BILAYER GRAPHENE

To elucidate which features of the anomalous tunnelling in graphene are related to the linear dispersion and which features are related to the pseudospin and chirality of the Dirac spectrum, it is instructive to consider the same problem for bilayer graphene. There are differences and similarities between the two graphene systems. Indeed, charge carriers in bilayer graphene have a parabolic energy spectrum as shown in Fig. 1c, which means they are massive quasiparticles with a finite density of states at zero energy, similar to conventional non-relativistic electrons. On the other hand, these quasiparticles are also chiral and described by spinor wavefunctions[20,21], similar to relativistic particles or quasiparticles in single-layer graphene. Again, the origin of the unusual energy spectrum can be traced to the crystal lattice of bilayer graphene with four equivalent sublattices[21]. Although 'massive chiral fermions' do not exist in the field theory, their existence in condensed-matter physics (confirmed experimentally[20]) offers a unique opportunity to clarify the importance of chirality in the relativistic tunnelling problem described by the Klein paradox. In addition, the relevant QED-like effects seem to be more pronounced in bilayer graphene and easier to test experimentally, as discussed below.

Charge carriers in bilayer graphene are described by an off-diagonal hamiltonian[20,21]

$$\widehat{H}_0 = -\frac{\hbar^2}{2m}\begin{pmatrix} 0 & (k_x - ik_y)^2 \\ (k_x + ik_y)^2 & 0 \end{pmatrix} \qquad (5)$$

which yields a gapless semiconductor with chiral electrons and holes with a finite mass m. An important formal difference between the tunnelling problems for single- and bi-layer graphene is that in the latter case there are four possible solutions for a given energy $E = \pm\hbar^2 k_F^2/2m$. Two of them correspond to propagating waves and the other two to evanescent waves. Accordingly, for constant potential V_i, eigenstates of hamiltonian (5) should be written as

$$\psi_1(x,y) = (a_i e^{ik_{ix}x} + b_i e^{-ik_{ix}x} + c_i e^{\kappa_{ix}x} + d_i e^{-\kappa_{ix}x}) e^{ik_y x}$$

$$\psi_2(x,y) = s_i\left(a_i e^{ik_{ix}x+2i\phi_i} + b_i e^{-ik_{ix}x-2i\phi_i} - c_i h_i e^{\kappa_{ix}x} - \frac{d_i}{h_i} e^{-\kappa_{ix}x}\right) e^{ik_y y}$$

where

$$s_i = \mathrm{sgn}\,(V_i - E); \quad \hbar k_{ix} = \sqrt{2m|E - V_i|}\cos\phi_i;$$
$$\hbar k_{iy} = \sqrt{2m|E - V_i|}\sin\phi_i$$
$$\kappa_{ix} = \sqrt{k_{ix}^2 + 2k_{iy}^2}; \quad h_i = \left(\sqrt{1 + \sin^2\phi_i} - \sin\phi_i\right)^2.$$

To find the transmission coefficient through barrier (2), we should set $d_1 = 0$ for $x < 0$, $b_3 = c_3 = 0$ for $x > D$ and satisfy the continuity conditions for both components of the wavefunction and their derivatives. For the case of an electron beam that is incident normally ($\phi = 0$) and low barriers $V_0 < E$ (over-barrier transmission), we obtain $\psi_1 = -\psi_2$ both outside and inside the barrier, and the chirality of fermions in bilayer graphene does not manifest itself. In this case, scattering at the barrier (2) is the same as for electrons described by the Schrödinger equation. However, for any finite ϕ (even in the case $V_0 < E$), waves localized at the barrier interfaces are essential to satisfy the boundary conditions.

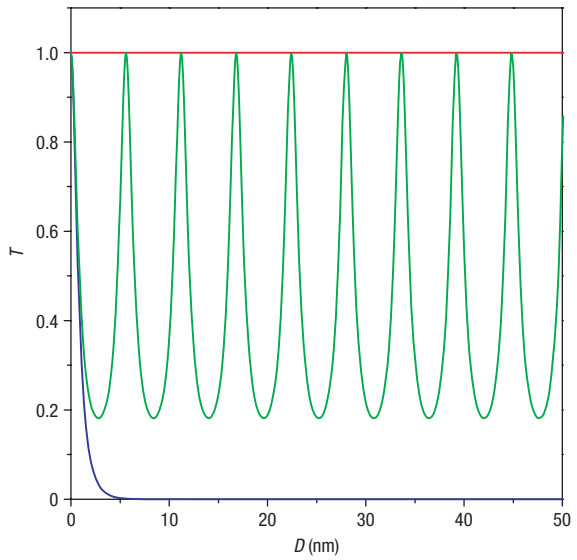

Figure 3 Chiral versus non-chiral tunnelling. Transmission probability T for normally incident electrons in single- and bi-layer graphene (red and blue curves, respectively) and in a non-chiral zero-gap semiconductor (green curve) as a function of width D of the tunnel barrier. Concentrations of charge carriers are chosen as $n = 0.5 \times 10^{12}$ cm^{-2} and $p = 1 \times 10^{13}$ cm^{-2} outside and inside the barrier, respectively, for all three cases. This yields barrier heights of ~450 meV for graphene and ~240 meV for the other two materials. Note that the transmission probability for bilayer graphene decays exponentially with the barrier width, even though there are plenty of electronic states inside the barrier.

The most intriguing behaviour is found for $V_0 > E$, where electrons outside the barrier transform into holes inside it, or vice versa. Examples of the angular dependence of T in bilayer graphene are plotted in Fig. 2b. They show a dramatic difference compared with the case of massless Dirac fermions. There are again pronounced transmission resonances at some incident angles, where T approaches unity. However, instead of the perfect transmission found for normally incident Dirac fermions (see Fig. 2a), our numerical analysis has yielded the opposite effect: massive chiral fermions are always perfectly reflected for angles close to $\phi = 0$.

Accordingly, we have analysed this case in more detail and found the following analytical solution for the transmission coefficient t:

$$t = \frac{4ik_1k_2}{(k_2 + ik_1)^2 e^{-k_2 D} - (k_2 - ik_1)^2 e^{k_2 D}}, \qquad (6)$$

where subscripts 1 and 2 label the regions outside and inside the barrier, respectively. The case of a potential step, which corresponds to a single p–n junction, is particularly interesting. Equation (6) shows that such a junction should completely reflect a normally incident beam ($T = 0$). This is highly unusual because the continuum of electronic states at the other side of the step is normally expected to allow some tunnelling. Furthermore, for a single p–n junction with $V_0 \gg E$, the following analytical solution

for any ϕ has been found:

$$T = \frac{E}{V_0}\sin^2(2\phi) \qquad (7)$$

which again yields $T = 0$ for $\phi = 0$. This behaviour is in obvious contrast to single-layer graphene, where normally incident electrons are always perfectly transmitted.

The perfect reflection (instead of the perfect transmission) can be viewed as another incarnation of the Klein paradox, because the effect is again due to the charge-conjugation symmetry (fermions in single- and bi-layer graphene exhibit chiralities that resemble those associated with spin 1/2 and 1, respectively)[20,21]. For single-layer graphene, an electron wavefunction at the barrier interface perfectly matches the corresponding wavefunction for a hole with the same direction of pseudospin (see Fig. 1a), yielding $T = 1$. In contrast, for bilayer graphene, the charge conjugation requires a propagating electron with wavevector k to transform into a hole with wavevector ik (rather than $-k$), which is an evanescent wave inside a barrier.

COMPARISON WITH TUNNELLING OF NON-CHIRAL PARTICLES

For completeness, we compare the results obtained with the case of normal electrons. If a tunnel barrier contains no electronic states, the difference is obvious: the transmission probability in this case is known to decay exponentially with increasing barrier width and height[22] so that the tunnel barriers discussed above would reflect electrons completely. However, both graphene systems are gapless, and it is more appropriate to compare them with gapless semiconductors with non-chiral charge carriers (such a situation can be realized in certain heterostructures[23,24]). In this case, we find

$$t = \frac{4k_x q_x}{(q_x + k_x)^2 e^{-iq_x D} - (q_x - k_x)^2 e^{iq_x D}},$$

where k_x and q_x are x-components of the wavevector outside and inside the barrier, respectively. Again, similar to the case of single- and bi-layer graphene, there are resonance conditions $q_x D = \pi N, N = 0, \pm 1, \ldots$ at which the barrier is transparent. For the case of normal incidence ($\phi = 0$), the tunnelling coefficient is then an oscillating function of tunnelling parameters and can exhibit any value from 0 to 1 (see Fig. 3). This is in contrast to graphene, where T is always 1, and bilayer graphene, where $T = 0$ for sufficiently wide barriers $D > \lambda$. This makes it clear that the drastic difference between the three cases is essentially due to different chiralities or pseudospins of the quasiparticles involved rather than any other feature of their energy spectra.

IMPLICATIONS FOR EXPERIMENT

The tunnelling anomalies found in the two graphene systems are expected to play an important role in their transport properties, especially in the regime of low carrier concentrations, where disorder induces significant potential barriers and the systems are likely to split into a random distribution of p–n junctions. In conventional 2D systems, strong enough disorder results in electronic states that are separated by barriers with exponentially small transparency[25,26]. This is known to lead to the Anderson localization. In contrast, in both graphene materials all potential barriers are relatively transparent ($T \approx 1$ at least for some angles) which does not allow charge carriers to be confined by potential barriers that are smooth on the atomic scale. Therefore, different electron and hole 'puddles' induced by disorder are not isolated but effectively percolate, thereby suppressing localization. This

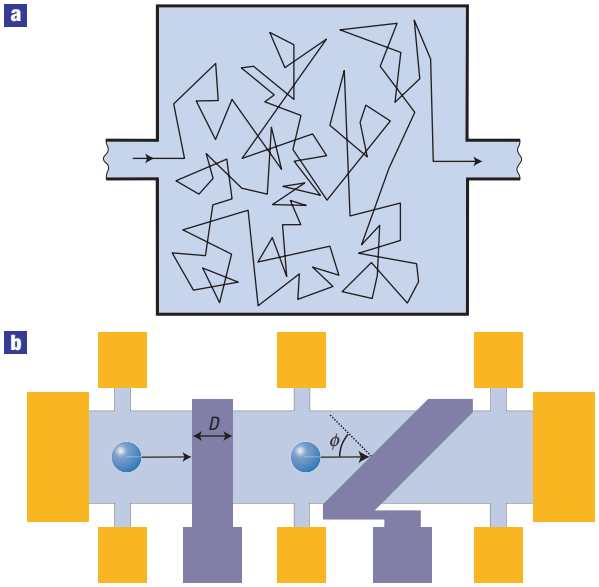

Figure 4 The chiral nature of quasiparticles in graphene strongly affects its transport properties. a, A diffusive conductor of a size smaller than the phase-coherence length is connected to two parallel one-dimensional leads. For normal electrons, transmission probability T through such a system depends strongly on the distribution of scatterers. In contrast, for massless Dirac fermions, T is always equal to unity due to the additional memory about the initial direction of pseudospin (see text). **b**, Schematic diagram of one of the possible tunnelling experiments in graphene. Graphene (light blue) has two local gates (dark blue) that create potential barriers of a variable height. The voltage drop across the barriers is measured by using potential contacts shown in orange.

consideration can be important for the understanding of the minimal conductivity $\approx e^2/h$ observed experimentally in both single-layer[13] and bilayer[20] graphene.

To further elucidate the dramatic difference between quantum transport of Dirac fermions in graphene and normal 2D electrons, Fig. 4a suggests a gedanken experiment where a diffusive conductor is attached to ballistic one-dimensional leads, as in the Landauer formalism. For conventional 2D systems, transmission and reflection coefficients through such a conductor are sensitive to detailed distribution of impurities and a shift of a single impurity by a distance of the order of λ can completely change the coefficients[27]. In contrast, the conservation of pseudospin in graphene strictly forbids backscattering and makes the disordered region in Fig. 4a always completely transparent, independent of disorder (as long as it is smooth on the scale of the lattice constant[17]). This extension of the Klein problem to the case of a random scalar potential has been proved by using the Lippmann–Schwinger equation (see the Supplementary Information). Unfortunately, this particular experiment is probably impossible to realize in practice because scattering at graphene's edges does not conserve the pseudospin[17,28]. Nevertheless, the above consideration shows that impurity scattering in the bulk of graphene should be suppressed compared with that of normal conductors.

The above analysis shows that the Klein paradox and associated relativistic-like phenomena can be tested experimentally using graphene devices. The basic principle behind such experiments would be to use local gates and collimators similar to those used in electron optics in 2D gases[29,30]. One possible experimental setup is shown schematically in Fig. 4b. Here, local gates simply cross the whole graphene sample at different angles (for example, 90°

and 45°). Intrinsic concentrations of charge carriers are usually low ($\sim 10^{11}$ cm^{-2}), whereas concentrations up to 1×10^{13} cm^{-2} can be induced under the gated regions by the bipolar electric field effect[9]. This allows potential barriers with heights up to $V_0 \approx 0.4$ eV and ≈ 0.23 eV for single- and double-layer samples, respectively. By measuring the voltage drop across the barriers as a function of applied gate voltage, their transparency for different V_0 can be analysed. Figure 2 shows that for graphene the 90° barrier should exhibit low resistance and no significant change in resistance with changing gate voltage. In comparison, the 45° barrier is expected to have much higher resistance and show a number of tunnelling resonances as a function of gate voltage. The situation should be qualitatively different for bilayer graphene, where local barriers should result in a high resistance for the perpendicular barrier and pronounced resonances for the 45° barrier.

Furthermore, the fact that a barrier (or even a single p–n junction) incorporated in a bilayer graphene device should lead to exponentially small tunnelling current can be exploited in developing graphene-based field effect transistors (FET). Such transistors are particularly promising because of their high mobility and ballistic transport at submicron distances[9,13,14]. However, the fundamental problem along this route is that the conducting channel in single-layer graphene cannot be pinched off (because of the minimal conductivity), which severely limits achievable on–off ratios for such FETs (ref. 9) and, therefore, the scope for their applications. A bilayer FET with a local gate inverting the sign of charge carriers should yield much higher on–off ratios.

Received 18 April 2006; accepted 20 June 2006; published 20 August 2006.

References

1. Klein, O. Die reflexion von elektronen an einem potentialsprung nach der relativistischen dynamik von Dirac. *Z. Phys.* **53,** 157–165 (1929).
2. Greiner, W., Mueller, B. & Rafelski, J. *Quantum Electrodynamics of Strong Fields* (Springer, Berlin, 1985).
3. Grib, A. A., Mamayev, S. G. & Mostepanenko, V. M. *Vacuum Effects in Strong Fields* (Friedmann, St-Petersburg, 1994).
4. Su, R. K., Siu, G. C. & Chou, X. Barrier penetration and Klein paradox. *J. Phys. A* **26,** 1001–1005 (1993).
5. Dombey, N. & Calogeracos, A. Seventy years of the Klein paradox. *Phys. Rep.* **315,** 41–58 (1999).
6. Calogeracos, A. & Dombey, N. History and physics of the Klein paradox. *Contemp. Phys.* **40,** 313–321 (1999).
7. Krekora, P., Su, Q. & Grobe, R. Klein paradox in spatial and temporal resolution. *Phys. Rev. Lett.* **92,** 040406 (2004).
8. Page, D. N. Hawking radiation and black hole thermodynamics. *New J. Phys.* **7,** 203 (2005).
9. Novoselov, K. S. *et al.* Electric field effect in atomically thin carbon films. *Science* **306,** 666–669 (2004).
10. Slonczewski, J. C. & Weiss, P. R. Band structure of graphite. *Phys. Rev.* **109,** 272 (1958).
11. Semenoff, G. W. Condensed-matter simulation of a three-dimensional anomaly. *Phys. Rev. Lett.* **53,** 2449–2452 (1984).
12. Haldane, F. D. M. Model for a quantum Hall effect without Landau levels: Condensed-matter realization of the 'parity anomaly'. *Phys. Rev. Lett.* **61,** 2015–2018 (1988).
13. Novoselov, K. S. *et al.* Two-dimensional gas of massless Dirac fermions in graphene. *Nature* **438,** 197–200 (2005).
14. Zhang, Y., Tan, Y. W., Stormer, H. L. & Kim, P. Experimental observation of the quantum Hall effect and Berry's phase in graphene. *Nature* **438,** 201–204 (2005).
15. Vonsovsky, S. V. & Katsnelson, M. I. *Quatum Solid State Physics* (Springer, Berlin, 1989) Sect. 4.6.6.
16. Boyanovsky, D., Blankenbecler, R. & Yahalom, R. Physical origin of topological mass in 2+1 dimensions. *Nucl. Phys. B* **270,** 483–505 (1986).
17. Ando, T., Nakanishi, T. & Saito, R. Berry's phase and absence of back scattering in carbon nanotubes. *J. Phys. Soc. Japan* **67,** 2857–2862 (1998).
18. McEuen, P. L., Bockrath, M., Cobden, D. H., Yoon, Y. G. & Louie, S. G. Disorder, pseudospins, and backscattering in carbon nanotubes. *Phys. Rev. Lett.* **83,** 5098–5101 (1999).
19. Tworzydlo, J., Trauzettel, B., Titov, M., Rycerz, A. & Beenakker, C. W. J. Quantum-limited shot noise in graphene. *Phys. Rev. Lett.* **96,** 246802 (2006).
20. Novoselov, K. S. *et al.* Unconventional quantum Hall effect and Berry's phase of 2π in bilayer graphene. *Nature Phys.* **2,** 177–180 (2006).
21. McCann, E. & Falko, V. I. Landau-level degeneracy and quantum Hall effect in a graphite bilayer. *Phys. Rev. Lett.* **96,** 086805 (2006).
22. Esaki, L. New phenomenon in narrow germanium para-normal-junctions. *Phys. Rev.* **109,** 603–604 (1958).
23. Meyer, J. R., Hoffman, C. A., Bartoli, F. J. & Rammohan, L. R. Type-II quantum-well lasers for the midwavelength infrared. *Appl. Phys. Lett.* **67,** 757–759 (1995).
24. Teissier, R. *et al.* Experimental determination of gamma-X intervalley transfer mechanisms in GaAs/AlAs heterostructures. *Phys. Rev. B* **54,** 8329–8332 (1996).
25. Ziman, J. M. *Models of Disorder* (Cambridge Univ. Press, Cambridge, 1979).
26. Lifshitz, I. M., Gredeskul, S. A. & Pastur, L. A. *Introduction to the Theory of Disordered Systems* (Wiley, New York, 1988).
27. Lee, P. A., Altshuler, B. L. & Webb, R. A. (eds) *Mesoscopic Phenomena in Solids* (North-Holland, Amsterdam, 1991).
28. Berry, M. V. & Mondragon, R. J. Neutrino billiards—time reversal symmetry-breaking without magnetic fields. *Proc. R. Soc. London A* **412,** 53–74 (1987).
29. Spector, J., Stormer, H. L., Baldwin, K. W., Pfeiffer, L. N. & West, K. W. Electron focusing in 2-dimensional systems by means of an electrostatic lens. *Appl. Phys. Lett.* **56,** 1290–1292 (1990).
30. Dragoman, D. & Dragoman, M. Optical analogue structures to mesoscopic devices. *Prog. Quantum Electron.* **23,** 131–188 (1999).

Acknowledgements

We are grateful to A. C. Neto, V. Fal'ko, P. Guinea and D. Khveshchenko for illuminating discussions. This work was supported by EPSRC (UK) and FOM (Netherlands).
Correspondence and requests for materials should be addressed to M.I.K.
Supplementary Information accompanies this paper on www.nature.com/naturephysics.

Competing financial interests

The authors declare that they have no competing financial interests.